

# Flawed Processing of Airborne EM Data Affecting Hydrogeological Interpretation

by Andrea Viezzoli<sup>1</sup>, Flemming Jørgensen<sup>2</sup>, and Camilla Sørensen<sup>3</sup>

---

## Abstract

Airborne electromagnetics (AEMs) is increasingly being used across the globe as a tool for groundwater and environmental management. Focus is on ensuring the quality of the source data, their processing and modeling, and the integration of results with ancillary information to generate accurate and relevant products. Accurate processing and editing of raw AEM data, the topic of this article, is one of the crucial steps in obtaining quantitative information for groundwater modeling and management. In this article, we examine the consequences that different levels of processing of helicopter transient electromagnetic method data have on the resulting electrical models and subsequently on hydrogeological models. We focus on different approaches used in the industry for processing of the raw data and show how the electrical resistivity–depth models, which is the end “geophysical” product (after data inversion) of an AEM survey, change with different levels of processing of the raw data. We then extend the study to show the impact on some of the hydrogeological parameters or models, which can be derived from the geophysical results. The consequences of improper handling of raw data to groundwater and environmental management can be significant and expensive.

---

## Introduction

In the past decade, the application of AEM data in hydrogeological investigations has steadily increased both in terms of areal coverage and also in complexity (e.g., Wynn 2002, 2006; English et al. 2004; Fitzpatrick and Clarke 2004; Paine and Minty 2005; Fitzpatrick and Munday 2007; Møller et al. 2009; Viezzoli et al. 2010). This in turn has led to an increased demand for the accurate resolution of the shape and the absolute value of the conductivity–depth structure of the ground. The intent has

been to extract important hydrogeological parameters in the subsurface, such as aquifer bounds, composition, and groundwater quality.

To address these demands, four main issues needed to be met, including the acquisition of data by better calibrated systems, the monitoring of the system at all times during acquisition, the appropriate processing of the derived raw data, and accurate inversion to model space that follows. This article focuses mainly on the third, and marginally the fourth, approached from an end user point of view, in this case the hydrogeologist or geologist.

Early airborne electromagnetic (AEM) systems were initially developed to assist in detecting mineralization, which could show up as anomalies in the measured voltage data. The system specifications were as a consequence not given as much considerations as nowadays, as the main consideration was how to achieve a high signal-to-noise (S/N) ratio so that the mineralization in the form of discrete conductors could be detected in the ground with more certainty.

---

<sup>1</sup>Corresponding author: Aarhus Geophysics Aps, C.F. Møllers Allé 4, Aarhus C 8000, Denmark; +393922979326; fax: +393922979326; av@aarhusgeo.com

<sup>2</sup>Geological Survey of Denmark and Greenland, GEUS, Lyseng Allé 1, DK-8270 Højbjerg, Denmark.

<sup>3</sup>Aarhus Geophysics Aps, C.F. Møllers, Allé 4, Aarhus C 8000, Denmark.

Received July 2011, accepted May 2012.

© 2012, The Author(s)

Ground Water © 2012, National Ground Water Association.

doi: 10.1111/j.1745-6584.2012.00958.x

AEM systems are constantly improved with increased sensitivity to small, shallow-intermediate (e.g., SkyTEM and new VTEM), and deeper (e.g., HeliTEM, Spectrem, and Tempest) features along with the use of a broader range of frequencies and different coil configurations. For a review of developments of some AEM systems in the past decade see Sattel (2009) or Paine and Minty (2005). Coupled with these developments, attempts are now being made to more accurately monitor system geometries to record navigation information and to better document and define ancillary information such as the actual waveform used in the survey. To some extent, this has become standard, although further work is required to make it completely routine. The relevance of modeling the system transfer function for accurate recovery of the ground conductivity structure through data inversion has recently been described (Christiansen et al. 2011).

The noteworthy improvement and better characterization of AEM systems, hardware specifications, and performance, both during the data acquisition and the data modeling, does not eliminate the necessity to pay particular attention to careful processing of the raw data. In fact, the latter also has significant influence on the derived conductivity–depth structure obtained through inversion, and therefore on the geological interpretation made from the derived conductivity–depth structure. This article highlights the potential implications (1) on the geophysical models of not thoroughly processing and assessing AEM data before inverting it and (2) how this might translate into erroneous hydrogeological interpretation obtained from the data. The main novelty and relevance lies mainly in Point 2 and in the systematic approach to illustrate Point 1. We argue that even though the end user of AEM products, be they a geologist or a hydrogeologist, does not need to be an expert in the employment of the methods described, it is appropriate for them to be aware of the different steps of the data processing techniques and their consequences for interpretation. We also hope to provide them with some tools to inspect the data critically and have the wherewithal to interact with AEM contractors in a constructive way.

We have used data from a small study area flown with the SkyTEM Time domain electromagnetic (EM) system (Sørensen and Auken 2004). The data were acquired in 2008 over an area in central Denmark (Figure 1).

We have devised a series of likely scenarios describing different levels of data processing, and we describe how the output model and interpretation is affected by them. Each investigation is described in detail in the following sections. First, we examine the results from a numerical and visual point of view in the model space, and then, where possible, we compare them with available borehole information. In the last section, we highlight the effects of the different processing steps on hydrogeological parameters such as aquifer thickness. Even though this article is focusing mainly on data processing, we also present results that illustrate the consequences of an inaccurate inversion.

## Method

### Time Domain Electromagnetic Surveying

The transient electromagnetic method (TEM) is based on the principle that the time varying magnetic field associated to a sharp turn off of current in a loop induces a current in the ground, whose decay over time is recorded by the instrument. A loop is used as transmitter coil (Tx) and another loop functions as the receiver loop (Rx). A current is transmitted in the Tx loop and is abruptly turned off. This generates an electromagnetic field, which will induce an electrical current in the surroundings, which in turn will induce a secondary magnetic field. The change in the secondary magnetic field with time ( $dB/dt$ ) is measured with the receiver coil and contains the information about the three-dimensional (3D) variability in electrical resistivity (conductivity) of the subsurface. The data are recorded in time windows or gates, and to increase the S/N ratio at late times, where the signal will have dissipated, the width of the gates increase at later times.

The  $dB/dt$  sounding curves that are measured at each sounding point can be inverted to recover a resistivity–depth model, which is consistent with the measured data. This is an iterative process of matching calculated forward responses of theoretical models to the actual measured response. Once a model fits the data, we have an indication of how the resistivity varies with depth at one specific sounding point. Several soundings, extracted either along a flight line or across lines, can form a stitched model section of the resistivity–depth models.

There are certain sources of noise associated with the method. One of the more significant ones is the influence of anthropogenic features such as power lines and fences, large metallic bodies, or anything that can carry a current. When acquiring data near these features, a magnetic field is not just induced in the ground, it is also induced in these features and they all contribute to the total measured response. In such circumstances, the measured data are said to be “coupled” to the infrastructure.

### SkyTEM AEM System

SkyTEM (Sørensen and Auken 2004) is a helicopter-based time domain AEM system. The transmitter loop is mounted on a lightweight frame (ca. 100 m<sup>2</sup>) and the receiver coils (x and z) are mounted at one end of this hexagonal frame, positioned such that the receiver coil is least affected by the primary field, that is, the self-response of the system. The frame is suspended from the helicopter and towed along in flight. The SkyTEM system uses a combination of two energizing magnetic moments, a low and a high one. The first uses higher current in the Tx loop, and provides information at greater depth, whereas the second one applies lower currents and faster turn off, hence is focused on the near surface.

### Survey Area

The survey area chosen for this study (Figure 1) forms part of a larger SkyTEM survey acquired in 2008.

This survey was conducted with a focus on the deeper geological features while simultaneously mapping near-surface structures. More specifically, the objectives were to map the aquifer's size and extent and their natural protection by clay layers.

The aquifers in this area are found within Miocene deltaic sand layers above conductive Paleogene clay layers. The Miocene sand layers are covered by a marine Miocene clay unit (the Gram Clay, Rasmussen et al. 2010), but buried Pleistocene valleys frequently cross-cut the entire Miocene setting (Jørgensen and Sandersen 2006). The sequence is capped by a relatively thin cover of glacial sediments, often composed of clay sediments such as clay till or lacustrine clay. To determine a measure of the aquifer vulnerability from surface pollutants, there was a need to map the thickness and extent of these near-surface glacial as well as Miocene clay layers.

The area chosen for this study was flown with line directions of SW-NE (Figure 1) and covers approximately 100 km<sup>2</sup>. A large number of power lines and roads are present in this area. Data collected close to these will be affected by them and need to be assessed and processed accordingly.

### Different Processing Levels

The following section describes the processing procedures that we believe are appropriate for extracting the most from the AEM data for hydrogeological purposes. These procedures aim at extracting most information about the subsurface from the data, while at the same time eliminating artifacts. They are described in detail in a study by Auken et al. (2009) and are the results of many years of experience in processing of AEM data for groundwater applications by many users in Denmark.

Processing procedures for editing data from any helicopter TEM system (e.g., SkyTEM, AeroTEM, or VTEM) before inverting them are commonly applied. Two

main processing steps are employed. These are (1) an automatic processing of Global Position System (GPS) locations, flight altitude, tilt of the transmitter frame, and the measured  $dB/dt$  data and (2) a manual processing as a quality analysis, quality control of the automatic step and further culling of coupled data.

The processing of the GPS, tilt, and altitude are primarily carried out automatically but will always require a manual check and a correction mainly to ensure that the automatic filters have been applied correctly, as well as to correct the editing if needed. The automatic processing of the  $dB/dt$  data is applied to remove coupling caused by man-made constructions, to average the raw data, and to automatically remove late time noise. The subsequent manual editing is primarily a visual control of the automatic processing and to correct any inadequacies of the automatic filters. Late time noise appearing in the data despite the averaging are also removed at this stage. Averaging the data improves the S/N ratio. Consequently the decoupling is carried out on the raw data while removal of late time noise is carried out on the averaged data.

### Results

#### Case 0: The "Raw" Data

Using AEM for hydrogeological applications is a natural progression after decades of using the method for mineral exploration. AEM data will occasionally be used in the raw form without processing or inverting it. We investigate whether raw unprocessed data can provide useful information.

The raw EM data are usually supplied with information about the AEM system's geometry (e.g., coil configurations, currents, effective area, calibration factors, low-pass filters, gate times, and a waveform description),

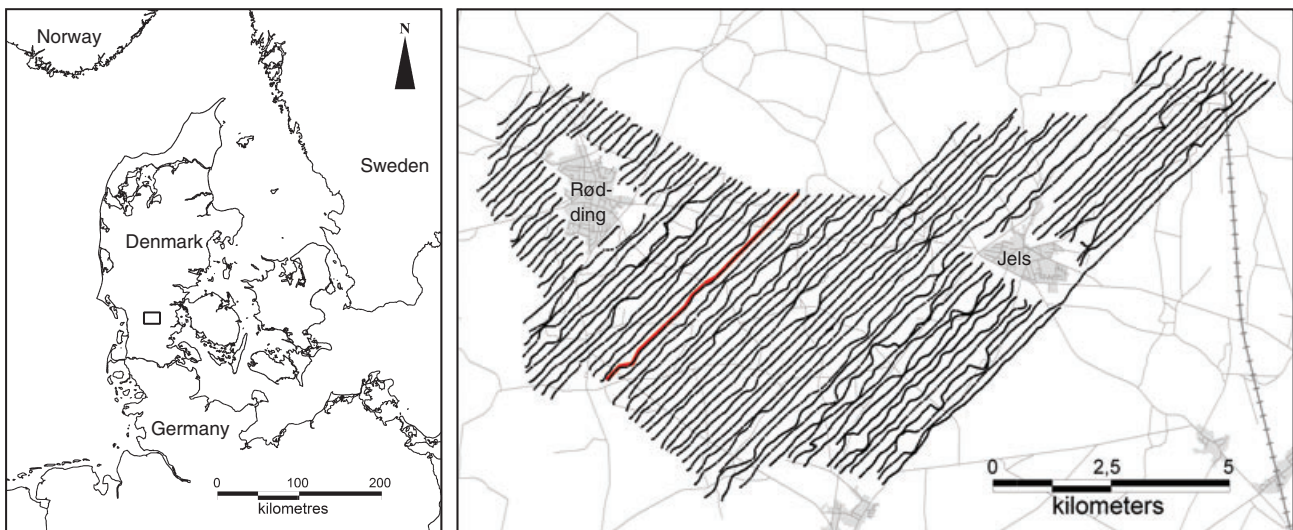


**Figure 1. Survey area and layout. The survey area is shown on the left map by a small rectangle. Urbanised areas, roads are shown together with the collected SkyTEM soundings on the right map. The red line shows the profile selected to present results also as vertical cross sections.**

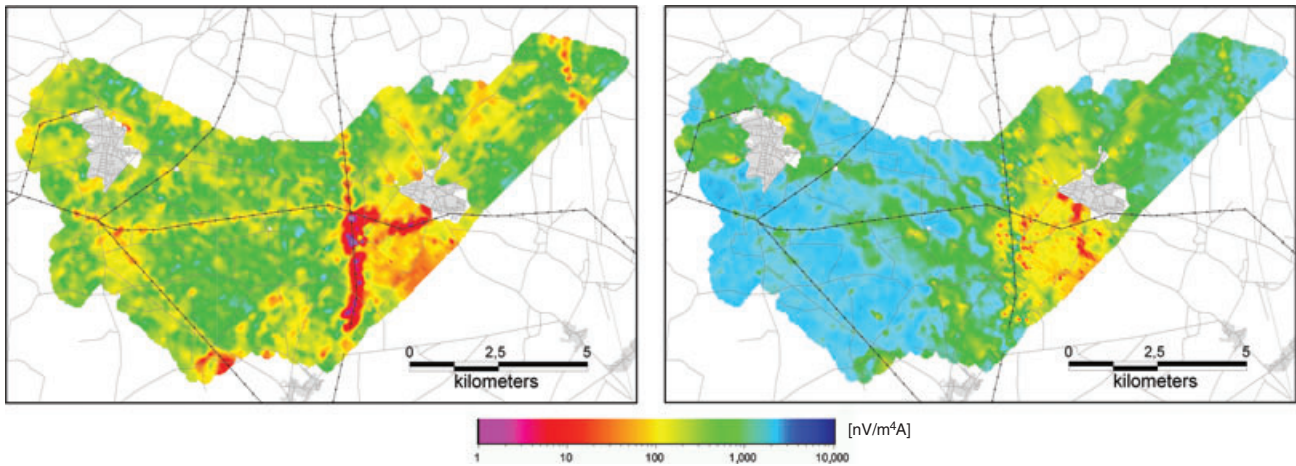


**Figure 2. Voltage maps describing raw signal received by the instrument. Left: Channel 7 low moment (about 90 microsec). Right: Channel 10 high moment (about 570 microsec). Voltage in nV/m<sup>4</sup>A. Grey segments represent main roads, while black segments with dots the main power lines in the area. Notice how they correspondent with anomalous voltage levels.**

the navigation data (e.g., GPS locations, altitude, and pitch and roll), and the EM data. The information supplied with the data is assumed to be correct. This is a crucial assumption as small changes in gate times, waveform, or filters can have a huge impact on the inversion results and therefore on the hydrogeological modeling (Christiansen et al. 2011).

We now investigate the usefulness of gridding the raw unprocessed  $dB/dt$  data, for instance, an early and a late time channel. Figure 2 shows the raw data for two different gridded time channels. The raw data primarily indicate whether there is a high or a low signal from the ground at a given time. However, the raw signal is also influenced significantly by the survey flying height and by a potential return signal from any metallic structures laid on or below the ground surface. So even though the raw data contain information of the ground response, one has to be able to distinguish between what is pure ground response and what is caused by altitude changes or coupling with infrastructures. Infrastructures aside, sounding by sounding, the early times represent qualitatively near-surface features and the late times represent features at greater depth. Even this assumption can be misleading, as the same time gate for two different soundings at different locations contains information about different depths, depending on the resistivity of the layers that the EM fields penetrate before reaching that given time. Summing up, raw data only show a spatial pattern of the measured response, which is heavily affected by flight height (or variability in other attitude parameters) and infrastructures and does not provide any direct information about conductivity or depth.

The gridded raw channels shown in Figure 2 show a near north-south running feature just to the right of the central part of the area. This feature correlates with a north-south trending power line at exactly that location. The higher signal is caused by coupling to man-made structures that affect those particular times (e.g., frequencies). Failing to acknowledge the presence of a

power line at that location could lead to interpretations suggesting “something” geological, often a conductor, hence clay or salty aquifers.

Figure 3 displays 3 min of SkyTEM data (high transmitter magnetic moment for the Cases 0/1, 2, and 3). Profiles of the raw data like this are an example of a common way to display the data when using AEM for mineral exploration. The top panel shows the raw EM data and two distinct features at time 14:36:20 and 14:37:20, which are due to coupling with metallic structures.

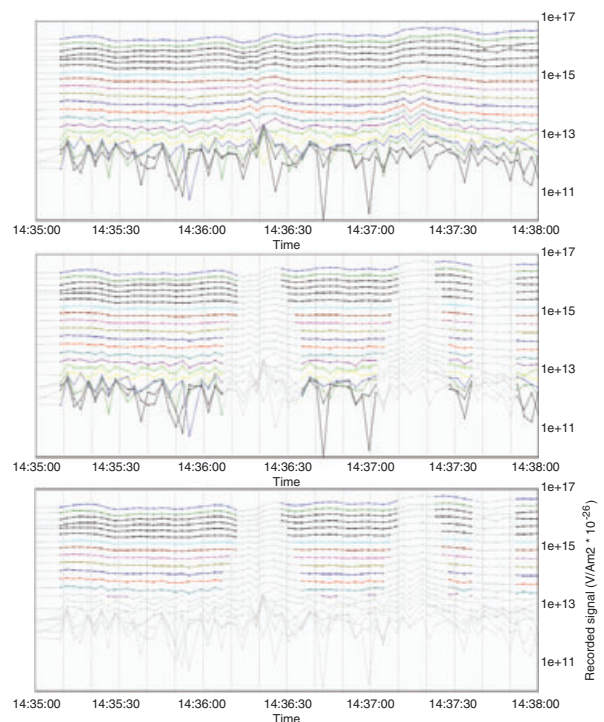


**Figure 3. Display of three minutes of EM data, (High moment time channels). Case 0 and 1 (raw data) in the top panel, Case 2 (decoupled data) in the middle panel, Case 3 (decoupled and denoised data), in the bottom panel.**

### Case 1: Inversion of Unprocessed Raw Data

The previous section showed that looking at the raw data, either gridded or in profiles, provides only information of signal levels and little information about electrical resistivities (conductivities) and depth. We need to invert the raw data to extract a conductivity depth structure.

The inversion applied is a full nonlinear inversion, based on an exact forward solution, using no lateral constraints. We discretize the subsurface in 19 layers with an increase in thickness with depth, performing a “smooth” or multilayer style inversion. Even though in this article we only show results from “smooth” inversions, they are largely applicable also to “blocky” inversions (few layers), which are often also carried out in hydrogeological applications. We will perform the same type of smooth inversion in all our cases. This kind of “true” inversion (i.e., not a data transform or an imaging procedure based

on approximations) arguably provides the accuracy in the results, which is required for hydrogeological applications. A depth of investigation (DOI), representing the local maximum depth to which there is sensitivity in the data about the subsurface, is also calculated. The DOI is discussed in details in a following section.

The first column of Figure 4 shows the results of an inversion of raw data, without applying any processing or filtering. The results are shown as resistivity slices at four selected depths: 20, 50, 110, and 180 m b.g.l. Other columns of the same figure refer to results of later cases, which are discussed in relevant sections.

The main features of the inversion result of Case 1 are as follows:

- The north-south trending feature corresponding to the power line, which was also seen in the gridded channel data (Case 0), becomes even more apparent. In the

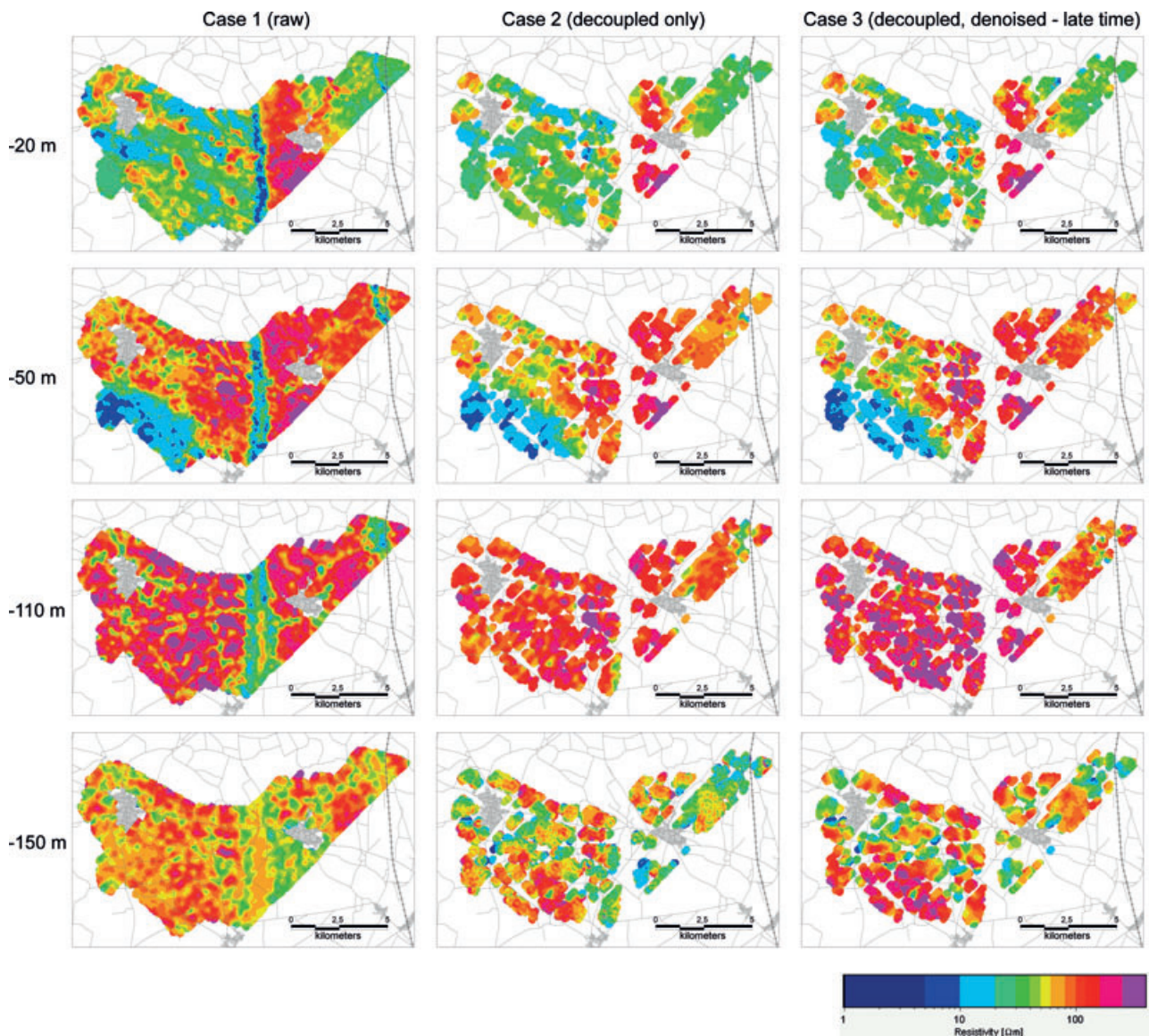
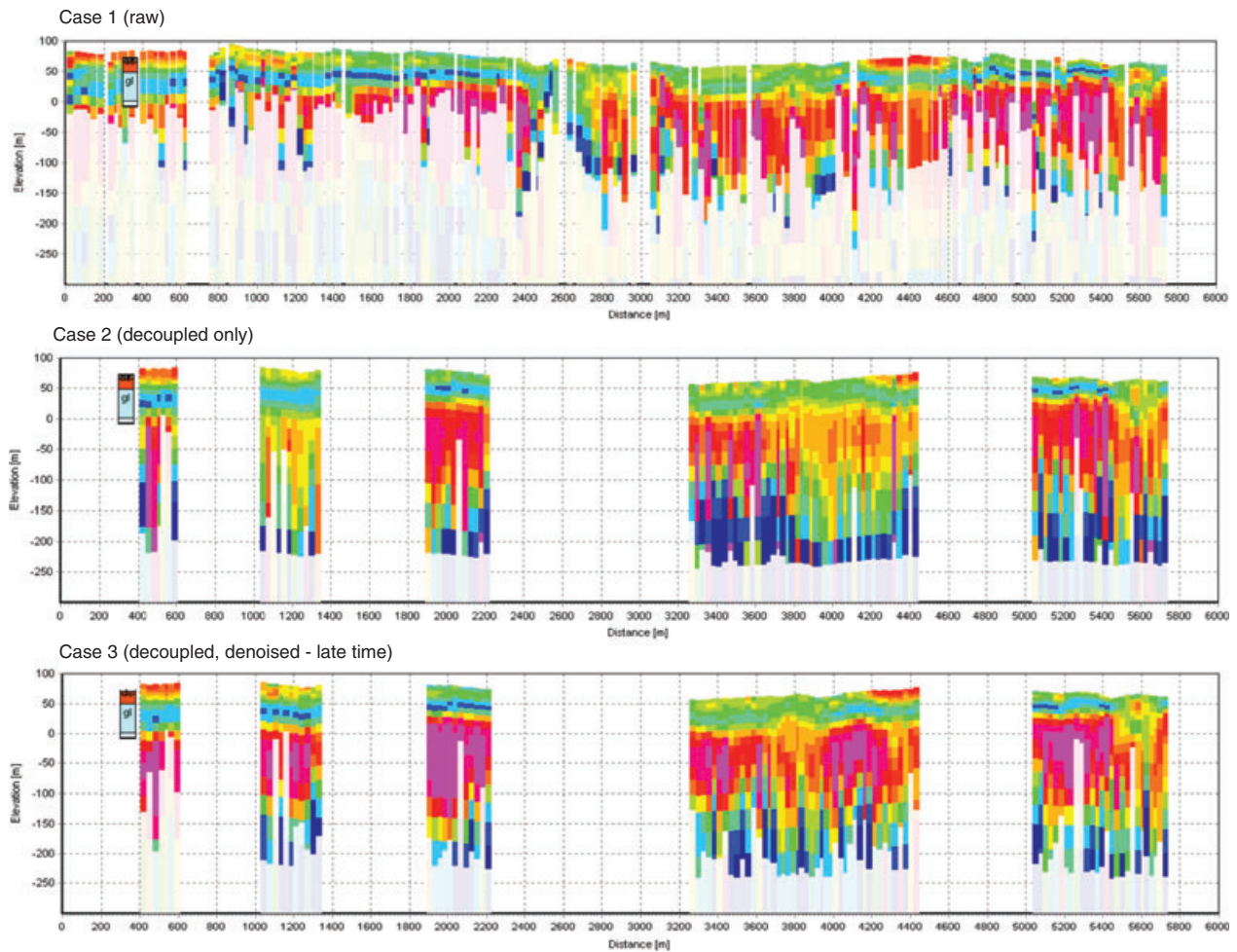


Figure 4. Resistivity slice maps obtained at 4 selected depths (20, 50, 110, 180 m b.g.l.) from inversion results of Case 1 (left column), Case 2 (middle column) and Case 3 (right column).



**Figure 5.** Resistivity cross section, for selected profile (see Fig. 1 for location), obtained from inversion results of different cases. Case 1 (top), Case 2 (middle panel), Case 3 (lower panel). Sections below DOI are shaded. Borehole on the left shows a superficial cover of sands and gravel (orange), overlying a clay layer (cyan) Borehole lithology: ks and gs = sands; gl = Gram clay.

near surface, it is seen as a relatively broad conductive feature, whereas at depth as a resistive narrow lineament sided by two more conductive areas.

- A correlation between roads and low-resistivity structures, especially in intermediate depth intervals.
- A spotted appearance in the deeper maps due to the lack of proper noise processing.

In areas with many cultural features, failure to remove couplings or late time noise will produce artifacts in the inverted model results. Coupling is a worry not only in Europe, in many parts of the world, such as the US and Canada, irrigation devices produce serious coupling in the data, even in rural areas with small roads and houses. The effect is less serious if the near surface is more conductive.

The results are also presented as vertical resistivity cross sections (Figure 5). The top panel shows the results of Case 1. The main points listed above can also be recognized in these cross sections. Notice the extent of the artificial conductors, the effect of the coupling, and the irregularity of the conductive layers, which could translate into hydrogeological units.

### Case 2: Decoupling of the Raw Data

After a careful automatic and manual decoupling of the EM data, an inversion using the same settings as previously is run. The middle panel in Figure 3 shows the decoupled data where data affected by cultural artifacts are removed (grey color).

In an area that contains a lot of infrastructure and, in general, moderate ground conductivity, removing all the noise caused by man-made sources can be difficult. Appropriate Geographic Information System (GIS) information from the area is crucial. Capacitive coupling (which produces a distinctive ringing shape in the TEM sounding) is much easier to recognize, than a galvanic coupling, which in the proximity of, for example, roads or power lines simply causes an increase of the signal in the whole measured sounding. Sudden altitude variations near these features will also often disguise this type of noise. In some cases, the best option is to edit the data, invert it, inspect the results, match them against available GIS, and assess whether any dubious features in the models seem to be caused by infrastructure. If that is the case, it is necessary to remove extra soundings close

to the source of noise. Preliminary knowledge of the geology in the area is beneficial in identifying such artifacts. In this case, the data were decoupled three times, before we were satisfied that no coupling was left in the data.

The inversion results of the final decoupled data set are presented as resistivity slices at different depths in the second column of Figure 4. By comparison with the results of Case 1 (raw data), it is clear that

- The north-south trending feature along the power line has been totally removed and therefore will not be misinterpreted.
- No correlation between conductors and roads or other infrastructures is present.
- The spotting at depth is still seen in the decoupled inversion results. This is expected, as these features are caused by ambient noise rather than coherent noise due to coupling with infrastructure.

The middle panel of Figure 5 shows the cross section, for the usual line profile, and confirms the main features discussed earlier.

### Case 3: Removing Late Time Noise

Removing the effects of infrastructure from the data is only the first step of data processing. The late time noise, which represents the effect of random ambient noise that becomes evident when the signal drops, also has to be assessed and dealt with. When the signal drops below the noise level, the slope of the  $dB/dt$  curve can typically be described by  $t^{-1/2}$  (for log time channels). The time gates that are only registering noise should therefore be deleted. Each individual sounding is assessed for this type of noise, and hence, the number of gates removed is not consistent over the entire survey. Let us refer to this procedure as “denoising.” The bottom panel, in Figure 3, shows the decoupled, denoised data (late time noisy data deleted, hence grayed out).

Inverting the data set with the late time noise present can cause artifacts in the deeper parts of the inverted models to be interpreted as conductors. Ignoring late time noise in multilayer (smooth) inversions, where vertical constraints are set between resistivities of layers, can also affect the intermediate part of the models, typically by decreasing its resistivity.

The third column of Figure 4 shows the inversion results of Case 3 in terms of resistivity at different depth slices. The main things to notice with respect to this and Case 2 are as follows:

- More uniform appearance at depth
- More resistive units, both at depth and at intermediate levels
- The near-surface results are similar

The vertical cross sections in the lower panel of Figure 5 also clearly show the effect of late time noise removal on the output models: The deeper parts of the models are confirmed to be less conductive, and

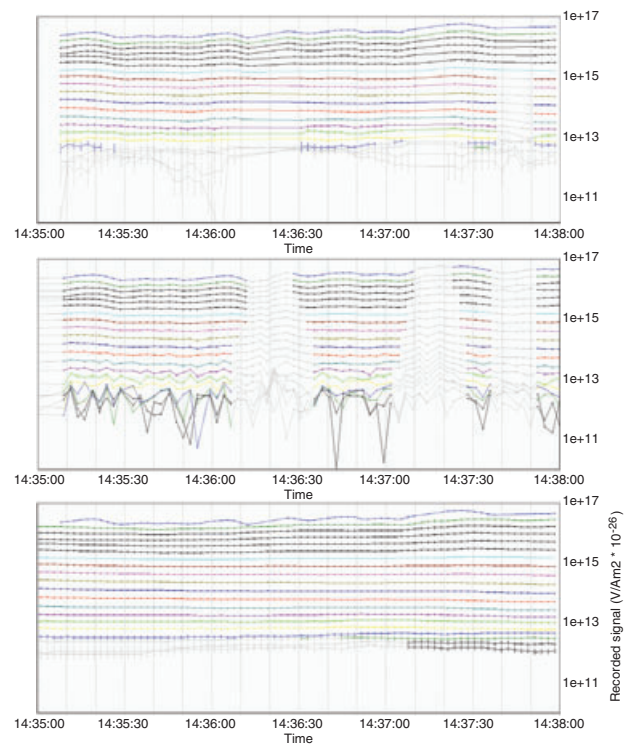
the intermediate layers become a bit more resistive, as expected. Also notice how the resistive intermediate unit, that is, the aquifer (Miocene sand), is thinner in Case 2. We discuss this in the dedicated section of the article.

### Cases 4 and 5: Applying Lateral Averaging

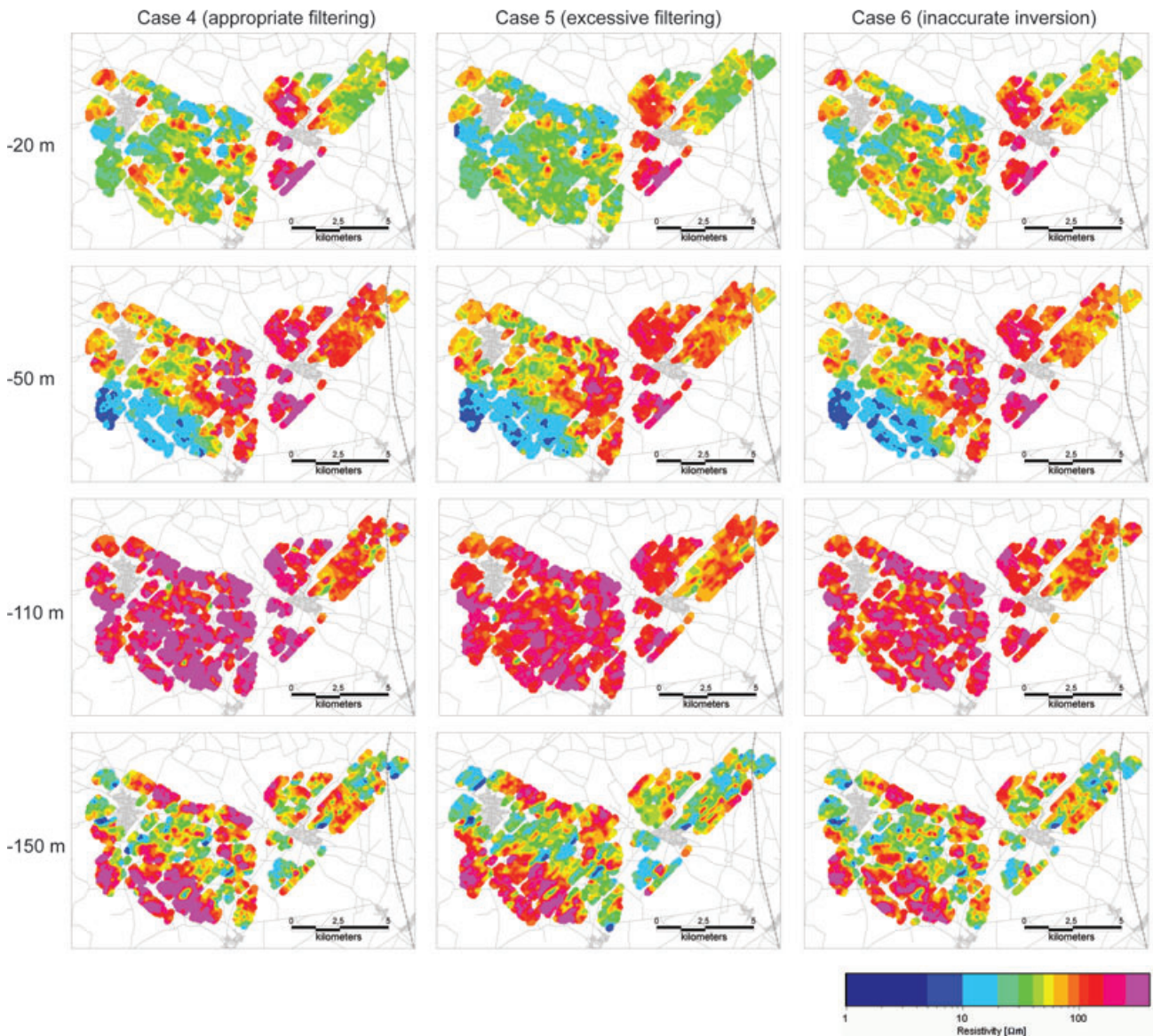
To increase the S/N ratio and consequently the DOI, it is relevant to apply lateral averaging filters to the EM responses before inversion. We apply trapezoid-shaped filters as described in detail in a study by Auken et al. (2009). This type of filtering, being narrow at early times and wider at late times, is designed to increase penetration depth without losing near-surface resolution. It also provides a noise value based on the statistics of the averaged data, for each time gate. The lateral averaging is added before the late time noise assessment and removal.

Figure 6 shows the effect of laterally averaging the High Moment data, for the same time interval as in Figure 3. The middle panel shows the effect on the data of moderate lateral filtering, that is, it preserves low-frequency features that have a geological cause, while reducing the high-frequency one, which are due to uncoherent, random background noise. The net effect is an increase in S/N ratio at late times. The bottom panel of Figure 6 shows the effect of excessive lateral filtering, which is discussed further toward the end of this section.

Figure 7 shows how the lateral averaging affects the inversion results in terms of resistivity slices at different depths. The left column refers to Case 4 (moderate filtering). The depth levels are the same as used in Figure 4;



**Figure 6.** The passage from decoupled data (top panel) to laterally averaged data for Case 4 (middle panel, moderate averaging) and Case 5 (lower panel, excessive averaging).



**Figure 7.** Resistivity slice maps obtained at 4 selected depths (20, 50, 110, 180 m b.g.l.) from inversion results of Case 4 (left column), Case 5 (middle column) and Case 6 (right column).

hence, they can be directly compared with, for example, the results obtained from Case 3. Figure 8 (top panel) shows the cross section for Case 4, for the usual selected profile.

A joint analysis of the maps and vertical sections highlights some similarities of the near-surface results between Cases 3 and 4. However, in Case 4

- The lateral averaging results in more spatially coherent models at depth, showing continuous structures.
- In addition, the DOI has increased.

This confirms that proper lateral filtering can provide better results at depth, without compromising the near-surface resolution.

It is not uncommon for clean (i.e., smooth) late time data to be perceived as proof of good quality AEM data. Therefore, AEM data providers might be tempted to push

hardware and software prefiltering to the limit (e.g., low-pass filters, spheric filters, stacking, and windowing). Data processors might do the same with software (e.g., lateral averaging) filtering techniques. However, if the filtering is too aggressive, there is a net loss of near-surface resolution, and artifacts may appear in the deeper part of the models. To illustrate this, we doubled the duration (i.e., the lateral dimension) of the trapezoid filter used previously, removed the late time noise, and inverted the data (we denote this in Case 5). The lower panel of Figure 6 shows the excessively smoothed data. The outcome of this procedure on the inversion results are presented in plane view in the middle column of Figure 7 and as cross sections in the middle panel of Figure 8. The main results of using too large lateral filters are as follows:

- Lower spatial variability of layer boundaries and resistivity values

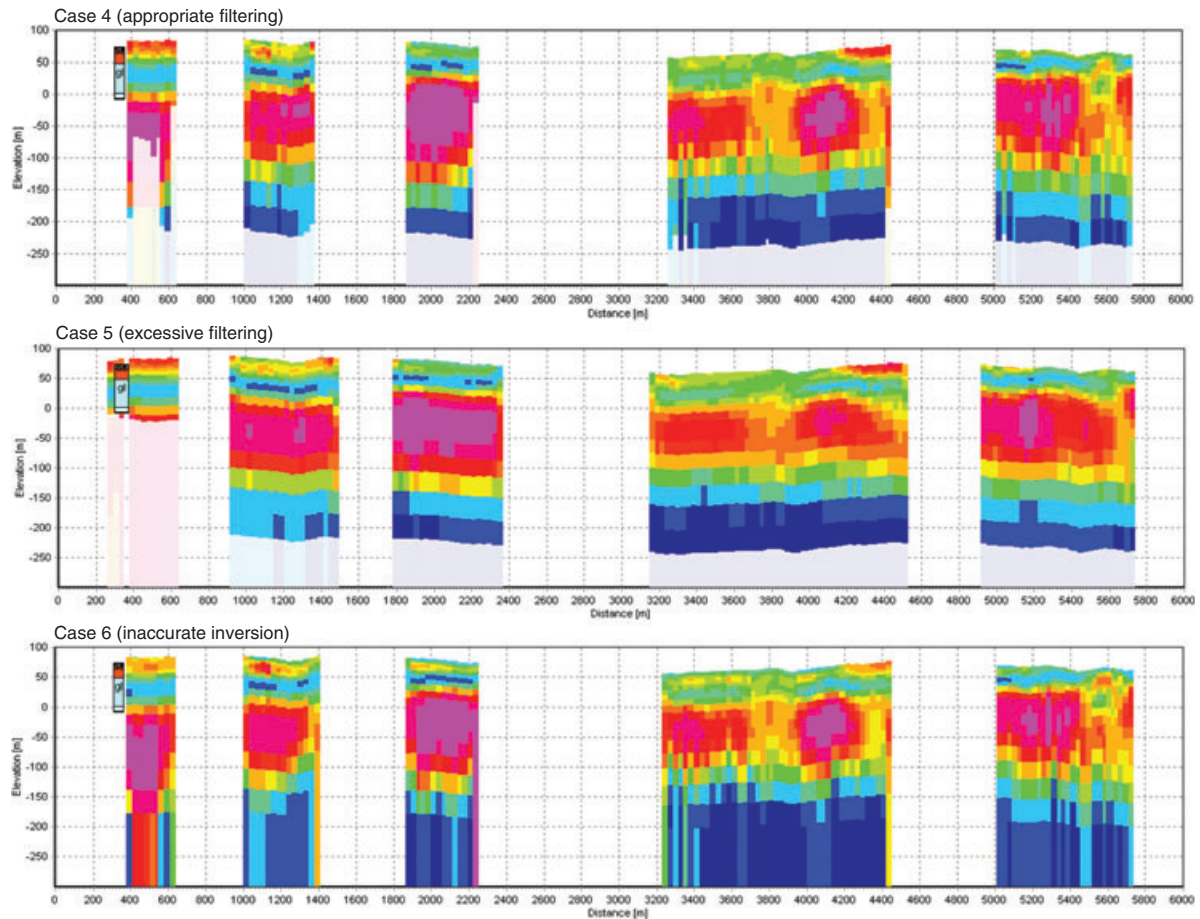


**Figure 8.** Resistivity cross section, for selected profile (see Fig. 1 for location), obtained from inversion of data from different cases. Case 4 (top), Case 5 (middle panel), Case 6 (lower panel). Sections below DOI are shaded. Borehole on the left shows a superficial cover of sands and gravel (orange), overlying a clay layer (cyan). Borehole lithology: ks and gs = sands; gl = Gram clay.

- Lower vertical variability of layer boundaries and resistivity values
- Elongated artifacts introduced in the deeper part of the model, in the direction of the flight lines.

These elongated features, which effectively smear the different units, are occasionally seen in AEM results and can be caused, among others, by this type of filtering. To avoid the excessive filtering and to obtain an increase in the resolution of the deeper part of the models, spatial constraints can be applied to the inversion (Viezzoli et al. 2008).

### Case 6: On the Effects of Inaccurate Inversion

The main focus of this article is on data processing rather than data inversion. Therefore, we have so far not discussed the consequences that inaccuracies in the inversion (i.e., improper modeling of different parameters of the system transfer function—the AEM system) have on the hydrogeological modeling obtained from interpretation of large AEM surveys. Christiansen et al. (2011) have shown the consequences of such inaccuracies on individual resistivity models. Their conclusions, on how inaccuracies when modeling different parameters

affect the recovered resistivity models, can be extrapolated to large data sets. We want thus to briefly illustrate the potential consequences for geophysical, and later, hydrogeological interpretations. We have therefore taken the data set from Case 4 (proper processing, late time noise assessment, and lateral filtering, i.e., our reference “perfect” processing) and reinverted it using a slightly wrong—yet plausible—description of two parameters of the system transfer function (Tx-Rx timing and gain). Figures 7 (right column) and 8 (lower panel) show the effect of these inaccuracies on the inverted models. Generally, the models become slightly more conductive, or the conductors are positioned a little bit closer to surface than in reality.

### Comparison with Borehole Information

Instead of exclusively looking at inverted maps and sections, we also compare the results to boreholes with lithological logs from the area. This is a complicated task due to varying borehole quality, scarcity of deep boreholes near flight lines, and the fact that we are comparing indirect measured resistivity values to a more “direct” lithological description.

Figures 5 and 8 show a rather shallow borehole (at 350 m), with lithological description, projected onto the profile. We do not expect the near-surface layers to be much affected by the different processing approaches, and all the inversions from all the cases should therefore match the borehole log quite well. Thus, a good agreement is seen for all Cases 1 to 5. For Case 6 (lower panel of Figure 8), on the other hand, some differences within this depth range could be expected. In fact, the vertical interface between sand (high resistivity) and clay (low resistivity) is less sharp in this case than in all the others and the match with the borehole slightly poorer.

We have also compared the one-dimensional resistivity models from Cases 2 and 4, and the lithological logs of another, deeper borehole, located at a distance of 140 m from the nearest soundings. Figure 9 shows how, as expected, Case 4 (lower panel) provided a better match to the borehole than Case 2 (upper panel). This is particularly true for the depth to the two main clay layers (units “mL” and “gL”), and to the underlying sands (units “ks/gS”), which in the resistivity models are seen from top to bottom, as conductive, more conductive, and then resistive.

### Hydrogeological Consequences of Different Processing Strategies

In this section, we illustrate the effects of the different processing approaches on the derived hydrogeological understanding of the area.

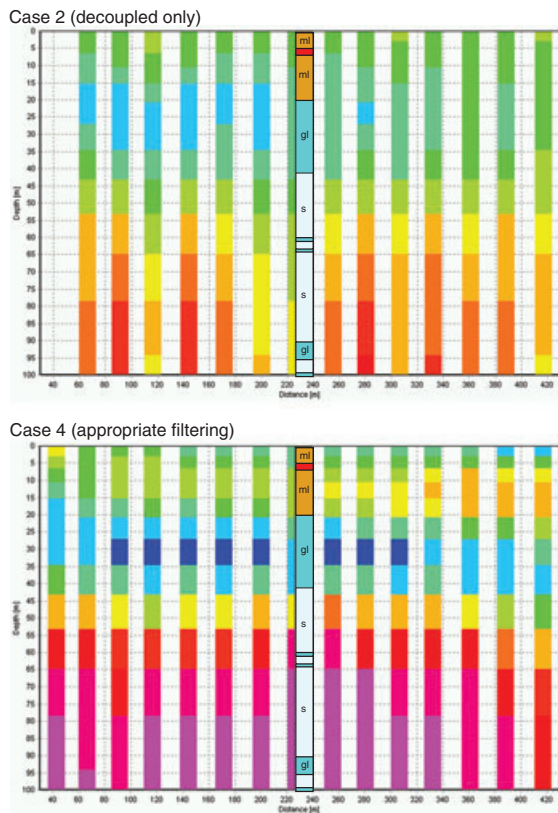


**Figure 9. Comparison between 1D resistivity models from Case 2 and Case 4, and the deep borehole. Borehole lithology: ml = clay till; s = sand/silts; gl = Gram clay.**

The resistivity maps, such as those presented in Figures 4 and 7, can be used directly to derive the approximate spatial variability of the hydrogeological units. For example, the resistivity–depth slice at 110-m depth describes the resistivity of the permeable sandy units associated with the deep Miocene aquifer present across the entire area at this depth. The resistivity–depth slice resulting from inverting without decoupling the data (Case 2) shows that resistivity values generally around or below 100  $\Omega\text{m}$  is indicative of fine- to medium-grained sediment or coarse-grained sediments with intervening clay layers or pore water of medium freshness. The resistivity values for Case 4 are generally higher (mainly  $>200 \Omega\text{m}$ ), implying coarser sediments, less intervening clay layers, and fresher groundwater. Without removing the late time noise (Case 2), the resistivity maps suggest that the aquifer would not have a very high yield. This is caused by a false assumption of a relatively high clay content or intervening clay layers in the aquifer. The other option is that the aquifer may possibly be affected by a slightly elevated salt content (decreasing the resistivity). The consequence could be that the aquifer would be disregarded as a potential resource for drinking water. If the spotted appearance of the raw data (Case 1) at this depth (in the aquifer) is not acknowledged as being artifacts, it could result in the setting being interpreted as spatially heterogeneous and interrupted by, for example, erosion of buried valleys or by glaciotectonics. Such processes would in turn have produced a complicated hydraulic system that would end up in a flow model unable to predict correct flow pathways (e.g., Shaver and Pusc 1992; Seifert et al. 2008).

Inversion results can be used to determine the geometry of the aquifers or to derive some other hydrogeologically relevant parameter such as groundwater salinity, salt balance, and aquifer vulnerability (e.g., Fitzpatrick and Munday 2007; Abraham et al. 2010; Kirkegaard et al. 2011). Figure 10 collects a series of derived maps obtained from extracting parameters from the inversion results using different search criteria. The top row shows the depth to the Paleogene clay, which, in this area, represents the bottom of the aquifer. The Paleogene clay is very conductive and there is an overall correlation between the deep good conductor in the surrounding soundings and the clay as found in deep boreholes. The maps of the Paleogene clay depth shown in Figure 10 were thus obtained by extracting the depth of the deep good conductor. The figure shows how the lack of late time noise removal (Case 2) produces a significant overestimate of the depth to this layer. Consequently, difficulties in establishing a proper 3D hydrogeological model occur.

The second row shows the cumulative thickness of the deep resistive unit, representative for the deep aquifer. The coupled data from Case 1 would perhaps suggest the presence of a clay-filled valley cutting through the aquifers or the upwelling of deep residual saline groundwater along a fault. The consequences of the first assumption would be that the flow regime of the entire survey area would be totally miscalculated in a flow model,

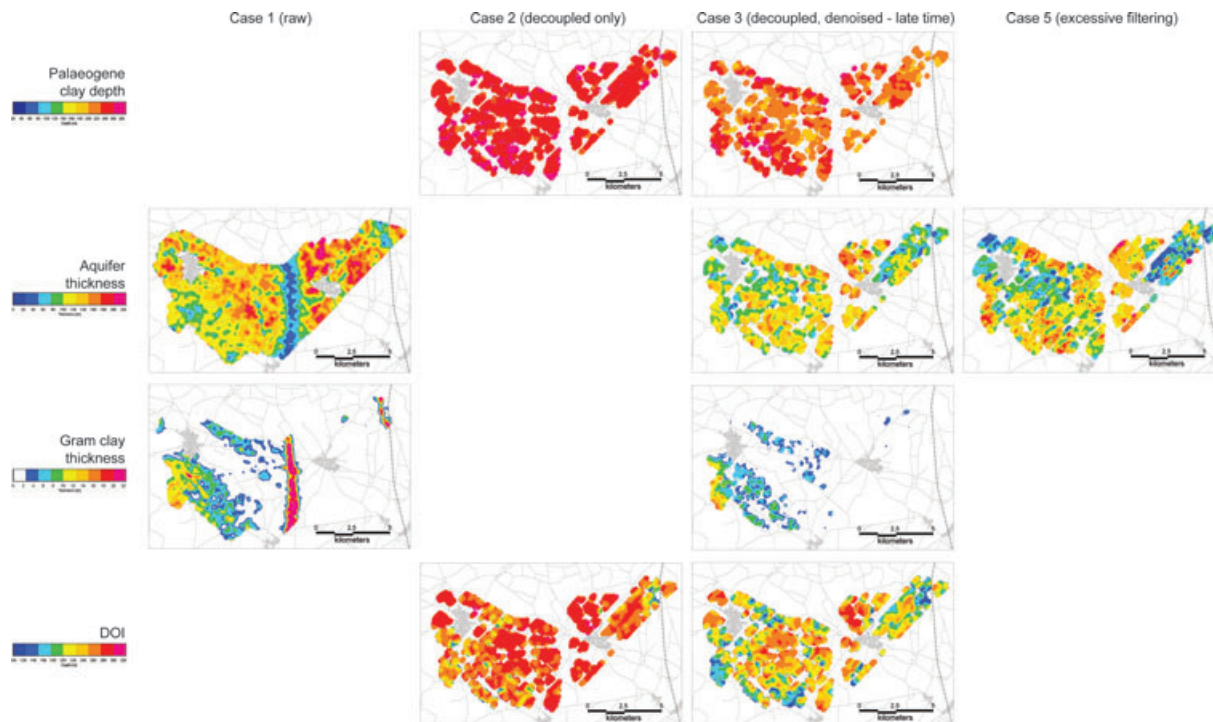


**Figure 10.** A sample of maps of direct hydrogeological applicability, derived from the geophysical results obtained in the different cases. Refer to the text for a description of the different maps. Case 1, 2, 3 and 5, from left to right.

since the hypothesized clay fill would effectively form a barrier to flow across the area. Also, no local groundwater resources would be expected to be present in this particular belt through the area, and potential groundwater abstraction here would be ruled out. Thus, local abstraction for drinking water or irrigation would imply unnecessary construction of pipelines to wells situated off the belt.

The excessive lateral filtering (Case 5) results in a clear lineation of the aquifer in the direction of flight. This could be mistaken as if the setting is very heterogeneously constructed giving rise to misinterpretations such as later erosion of valleys or the occurrence of heavy tectonism leading to erroneous 3D models and thus also flow models.

The aquifer thickness varies by many tens of meters depending on the processing undertaken. Without processing the data, the modeled aquifer is much thicker than after processing, with the consequence that, for a given porosity, the amount of abstractable groundwater resources for the area could be overestimated.

The third row in Figure 10 shows a map of thickness of the Gram Clay. The Gram Clay (Rasmussen et al. 2010) is a tertiary marine clay formation, partly present in the area close to the surface. It corresponds to the clay layer described in both boreholes (Figures 5, 8, and 10) at depths of about 20 m. The clay overlies the deep aquifer and can thus be extended into a map of vulnerability, because the lack of clay cover puts them at risk from surface pollution (e.g., Thomsen et al. 2004). Cases 1 and 3 show quite different results and would possibly result in indifferent management approaches and decisions. Apart

from the difference given by the north-south artifact clearly visible in Case 1, a general overestimation of the clay thickness in Case 1 with respect to Case 3 is seen. The discontinuity of the clay cover that occurs after processing can represent potentially a bigger issue. Several small areas reveal a lack of the protecting Gram Clay, which gives them a high priority within groundwater protection planning. These would be expected to serve as catchment zones for abstraction wells in the aquifer, and their location is thus very important.

## The Depth of Investigation

Even though not strictly a hydrogeological parameter, the DOI is useful for the user of AEM data (and of any other surface geophysical method). It defines an estimate of the depth below which the sensitivity of the methodology falls below a (given) acceptable threshold, and therefore, the resistivity models produced by the inversion are not trustworthy. There are different approaches for defining the DOI (sometimes referred to depth of penetration as well). We adopt the one by Christiansen and Auken (2010), based on the sensitivity matrix. It takes the number of data points and the errors associated with them into account. A DOI value should always be given with the results. We investigate how differences in the processing of the data affect the DOI.

The last row in Figure 10 reports the DOI obtained from Cases 2 and 3. The DOI is significantly and erroneously higher (>40 m) in Case 3, that is, when the noisy late time gates were not removed before the inversion. This is caused by the extra gates and by the enhanced

conductive features at depth, which can be the result of the late time noise as previously shown. These artificial conductors are usually well resolved, and therefore have a good sensitivity measure, which pushes the DOI deeper. Relying on AEM modeling results beyond the depth at which they really become unreliable can have consequences for groundwater resource management, caused by misinterpretation of data close to or below the DOI. An example could be if models show high resistivities at this depth, which can be correlated to the presence of deep-seated aquifers. This in turn may lead to a wrong assumption of having excess groundwater resources, and consequently, a potential overuse of the groundwater. It could also cause expensive but unsuccessful drilling for deep-seated groundwater.

## Discussion and Conclusions

AEM methods, like many other geophysical techniques, can be applied to quantitative hydrogeological investigations. When employed, it is an effective tool for groundwater and environmental management. However, accurate processing and editing of AEM data is one of the crucial steps involved in obtaining information appropriate to their effective and full use. Having the best source data, the best inversion procedures and most skilled hydrogeologists do not prevent a potential disappointing result. We have shown how different processing inaccuracies, or even just different approaches, can lead to incorrect geophysical results, which can then turn into misleading interpretations, wrong hydrogeological models, and non-effective management. Failing to remove data affected by infrastructure, poor noise assessment and removal, and excessive filtering are all issues that map directly to the model space, to the geological and hydrogeological parameters, and to the interpretation or modeling. The consequences can be many: low confidence in the derived models in general, overestimation of the depth to bedrock (or bottom of aquifer) by several tens of meters, excluding abstraction from good aquifers due to fake flow barriers, and posing the shallow aquifers at risk due to overestimation of the protecting impermeable layers. The impact, both environmentally and financially, can be severe.

We contend that, from a groundwater and environmental management perspective, the efforts and resources spent on proper processing of the AEM data are necessary to achieve the most out of a very effective methodology and to reduce the risk of possible misinterpretation of the final results.

## References

- Abraham, J.D., J.C. Cannia, S.M. Peterson, B.D. Smith, B.J. Minsley, and P.A. Bedrosian. 2010. Quantitative hydrogeological framework interpretations using helicopter electromagnetic surveys for the North Platte Valley, Western Nebraska groundwater model. *ASEG Sydney*, Extended abstract.
- Auken, E., A.V. Christiansen, J.H. Westergaard, C. Kirkegaard, N. Foged, and A. Viezzoli. 2009. An integrated processing scheme for high-resolution airborne electromagnetic surveys, the SkyTEM system. *Exploration Geophysics* 40: 184–192.
- Christiansen, A.V., and E. Auken. 2010. A global measure for depth of investigation in EM and DC modeling. *ASEG Sydney*, Extended abstract.
- Christiansen, A.V., A. Viezzoli, and E. Auken. 2011. Quantification of modeling errors in airborne TEM caused by inaccurate system description. *Geophysics* 76: F43–F52.
- English, P., P. Richardson, and M. Glover. 2004. Interpreting airborne electromagnetic data as an adjunct to hydrogeological investigations. In *Regolith 2004*. CRC LEME.
- Fitzpatrick, A., and J.D.A. Clarke. 2004. The potential of geophysics to map salt water intrusion in the Burdekin Delta. In *Regolith 2004*. CRC LEME.
- Fitzpatrick, A., and T. Munday. 2007. The application of airborne geophysical data as a means of better understanding the efficacy of disposal basins along the Murray River: An example from Stockyard Plains, South Australia. *ASEG Extended Abstracts*.
- Jørgensen, F., and P.B.E. Sandersen. 2006. Buried and open tunnel valleys in Denmark—Erosion beneath multiple ice sheets. *Quaternary Science Reviews* 25, no. 11–12: 1339–1363.
- Kirkegaard, C., T. Sonnenborg, E. Auken, and F. Jørgensen. 2011. Salinity distribution in heterogeneous coastal aquifers mapped by airborne electromagnetics. *Vadose Zone Journal* 10: 125–135.
- Møller, I., V.H. Søndergaard, F. Jørgensen, E. Auken, and A.V. Christiansen. 2009. Integrated management and utilization of hydrogeophysical data on a national scale. *Near Surface Geophysics* 7: 647–659.
- Paine, J.G., and B.R.S. Minty. 2005. Airborne hydrogeophysics. In *Hydrogeophysics*, 333–360. The Netherlands: Springer.
- Rasmussen, E.S., K. Dybkjær, and S. Piasecki. 2010. Lithostratigraphy of the Upper Oligocene-Miocene succession of Denmark. *Geological Survey of Denmark and Greenland Bulletin* 22: 92.
- Sattel D. 2009. An overview of helicopter time-domain EM systems. *ASEG Extended Abstracts 2009*.
- Seifert, D., T.O. Sonnenborg, P. Scharling, and K. Hinsby. 2008. Use of alternative conceptual models to assess the impact of a buried valley on groundwater vulnerability. *Hydrogeology Journal* 16, no. 4: 659–674.
- Shaver, R.B., and S.W. Pusc. 1992. Hydraulic barriers in pleistocene buried-valley aquifers. *Ground Water* 30: 21–28.
- Sørensen, K.I., and E. Auken. 2004. SkyTEM—A new high-resolution helicopter transient electromagnetic system. *Exploration Geophysics* 35: 191–199.
- Thomsen, R., V.H. Søndergaard, and K.I. Sørensen. 2004. Hydrogeological mapping as a basis for establishing site-specific groundwater protection zones in Denmark. *Hydrogeology Journal* 12, no. 5: 550–562.
- Viezzoli A., E. Auken, A.V. Christiansen, and T. Munday. 2010. Accurate quasi 3D versus practical full 3D inversion of AEM data: The Bookpurnong case study. *Preview* 149: 23–31.
- Viezzoli, A., A.V. Christiansen, and E. Auken. 2008. Quasi-3D modeling of airborne TEM data by spatially constrained inversion. *Geophysics* 73: F105–F113.
- Wynn, J. 2002. Evaluating groundwater in arid lands using airborne magnetic/EM methods. An example in the southwestern U.S. and northern Mexico. *The Leading Edge* 21: 62–64.
- Wynn, J. 2006. Mapping ground water in three dimensions—An analysis of airborne geophysical surveys of the Upper San Pedro River Basin, Cochise County, Southeastern Arizona. *USGS Professional Paper 1674*.